Structural polymorphism of a cytosine-rich DNA sequence forming i-motif structure: Exploring pH based biosensors

Saami Ahmed, Mahima Kaushik, Swati Chaudhary, Shrikant Kukreti

PII: S0141-8130(17)34857-2
DOI: https://doi.org/10.1016/j.ijbiomac.2018.01.053
Reference: BIOMAC 8885

To appear in:

Received date: 7 December 2017
Revised date: 5 January 2018
Accepted date: 9 January 2018

Please cite this article as: Saami Ahmed, Mahima Kaushik, Swati Chaudhary, Shrikant Kukreti , Structural polymorphism of a cytosine-rich DNA sequence forming i-motif structure: Exploring pH based biosensors. The address for the corresponding author was captured as affiliation for all authors. Please check if appropriate. Biomac(2017), https://doi.org/10.1016/j.ijbiomac.2018.01.053

Structural polymorphism of a Cytosine-rich DNA Sequence forming i-motif structure: Exploring pH based biosensors

Saami Ahmed[a], Mahima Kaushik[b], Swati Chaudhary[a], Shrikant Kukreti[a]*

[a]Nucleic Acids Research Lab, Department of Chemistry, University of Delhi, Delhi-110007

[b]Cluster Innovation Center, University of Delhi, Delhi-110007

E-mail: skukreti@chemistry.du.ac.in; kukretishrikant@yahoo.com

Corresponding Author:
Prof. Shrikant Kukreti
Department of Chemistry,
University of Delhi, Delhi, India

Key words: i-motif, cytosine-rich sequences, pH-based biosensors, nano-biosensor, structure-specific recognition by biosensors, DNA structural polymorphism

Abstract

Sequence recognition and conformational polymorphism enable DNA to emerge out as a substantial tool in fabricating the devices within nano-dimensions. These DNA associated nano devices work on the principle of conformational switches, which can be facilitated by many factors like sequence of DNA/ RNA strand, change in pH or temperature, enzyme or ligand interactions etc. Thus, controlling these DNA conformational changes to acquire the desired function is significant for evolving DNA hybridization biosensor, used in genetic screening and molecular diagnosis. For exploring this conformational switching ability of cytosine-rich DNA oligonucleotides as a function of pH for their potential usage as biosensors, this study has been designed. A C-rich stretch of DNA sequence (5'-TCCCCCAATTAATTCCCCCA-3'; SG20c) has been investigated using UV-Thermal denaturation, poly-acrylamide gel electrophoresis and CD spectroscopy. The SG20c sequence is shown to adopt various topologies of i-motif structure at low pH. This pH dependent transition of SG20c from unstructured single strand to unimolecular and bimolecular i-motif structures can further be exploited for its utilization as switching on/ off pH-based biosensors.

Introduction

After the discovery of Watson and Crick B-form DNA double helix, ample investigations have been done on DNA structures [1]. It is now confirmed that DNA can adopt a varied range of conformations like A, B, C, Z forms along with multistranded DNA structures like triplex, i-motif and guanine quadruplex [2]. Guanine-rich sequences often exhibit the formation of G-quadruplex structure which are commonly found in telomeric and promoter regions of the gene [3-5]. These guanine-rich sequences also have their complementary C-rich stretches and hence studying them becomes equally important. These cytosine-rich sequences can form tetraplex like structures called as i-motifs. Biological importance and *in vivo* existence of such structures is still not much clear, yet a large number of studies to answer related questions are being carried out in various research labs. During i-motif formation, an ordered base stacking intercalation takes place, of two or more cytosine bases with $C{\bullet}C^+$ pairing. This DNA secondary structure can be formed by one, two or four C-rich strands. The acidic environment protonates some cytosines and thereby leads to the formation of cytosine-cytosine$^+$ base pairs. These $C{\bullet}C^+$ base pairs are responsible for the formation of i-motif structure under acidic conditions and were initially reported by Gehring, Leroy and Guéron in 1993 [6]. Formation of an intramolecular i-motif was also observed in human telomere segment [7]. Simplest topology of i-motif is one, where two parallel-stranded DNA duplexes are combined with each other in an antiparallel manner by intercalating its $C{\bullet}C^+$ base pair. Initially, i-motif at physiological conditions was considered as unstable moiety, however later, it was perceived that this is not always the case. Formation of i-motif structures depend on various factors like DNA oligonucleotide sequence and environmental conditions. Cytosine-rich sequences, because of their property to exhibit pH dependent folding and unfolding, are also widely used as pH switches in nanotechnology, which are utilized for designing nanomachines [8-11], logic operation switches [12-14] and to figure out the pH changes in living systems [15, 16].

Here in this study, we investigated the i-motif (C-tetraplex) forming potential of a C-rich sequence SG20c 5'-TCCCCCAATTAATTCCCCCA-3' at varied solution conditions. To check the purity of the sequence, urea containing denaturation PAGE was performed prior to checking the structural status. The structural status and stability of SG20c at neutral and acidic pH was determined by non-denaturating gel electrophoresis, UV-thermal denaturation and circular dichroism (CD) studies.

Materials and Methods:

The studied DNA oligonucleotides were procured commercially from Bio Basic Inc., Canada. These were synthesized on 1 μM scale. The purity of the oligomer was cross checked by running them on 20 % PAGE containing 7M urea and the presence of single band in gel image reflected its purity. The DNA oligonucleotides were stored at -20°C. The stock solutions were prepared by dissolving the lyophilized oligonucleotide powder in MilliQ water. By employing the nearest neighbor method, the extinction coefficients (ε) were determined, which were further utilized to analyze the concentration of studied oligonucleotides at 260 nm, spectrophotochemically [17]. Various deoxyoligonucleotides and used markers (*) with their respective ε values are tabulated below (**Table. 1)**:

S.No	**DNA Oligonucleotides**	**ε [M^{-1} cm^{-1}]**
1.	d-TCCCCCAATTAATTCCCCCA -(SG20c)	178,600
2.	d-TGGGGGAATTAATTGGGGGA -(SG20)	207,200
3.	d-CTTGAGCTCAAG-(PAL12)*	113,700
4.	d-CTTGAGCTTGAGCTCAAGCTCAAG-(PAL24)*	226,100
5.	d-GACTGACTTAAGCGCATAGCTAGCTAGCTCGATAGCTGA-(M35)*	342,600
6.	d-TCAGCTATCGAGCTAGCTAGCTATGCGCTTAAGTCAGTC-(M35c)*	333,100

UV-thermal denaturation:

For performing UV-thermal denaturation analysis, Varian make CARY-100 Spectrophotometer was used, which was equipped with peltier programmer. The quartz cuvette with 10 mm optical path length having volume capacity of 110 μl solution was used. By taking an appropriate range of strand concentrations, the DNA samples were prepared. The prepared samples were allowed to heat up to 100 °C for 5 minutes and then were allowed to cool to room temperature by slow cooling. The absorbance of the samples was measured at 265 nm and 295 nm wavelengths as a function of temperature. The temperature was increased from 20 to 95 °C with a pace of 0.5 °C/ min. The sample solution was tightly capped to prevent any evaporation. The absorbance versus temperature profiles was normalized and their first derivative curves were

plotted, whose peak maxima gave the thermal melting (T_M) value. The reported T_M has an accuracy of +/- 1 °C.

Circular dichroism:

CD scans were recorded using JASCO-715 spectropolarimeter, at a scanning rate of 100 nm/ min from 200 to 320 nm wavelength. Here, a quartz cuvette of 10 mm path length and 1 ml volume was used. The samples prepared were incubated overnight at 4 °C. The average CD scans of the DNA samples were subtracted from the buffer scan at room temperature. Further, the CD Data was normalized as a function of DNA strand concentration. The normalized CD data is then plotted against the range of wavelength for getting a CD curve.

Native polyacrylamide gel electrophoresis:

15 % (w/v) polyacrylamide gel was used for performing native gel experiments. The DNA oligonucleotide samples were prepared in sodium cacodylate buffer (pH 7.4 and 5.2) at desired concentrations. The total volume of sample for non-denaturating gel was 20 µL. These samples were heated at 95 °C for 5 mins and then allowed to slowly cool down to room temperature. The DNA oligonucleotide samples were incubated overnight at 4 °C. The gel samples had sodium cacodylate buffer, NaCl and EDTA at a concentration of 20 mM, 100 mM and 0.1 mM respectively. The running buffer consisted of 1X TBE of 7.4 pH and 5.2 pH having same concentration of salt and chelating agent EDTA as in gel and sample. The gel experiments were performed at constant 65V, in the cold room. For tracking the movement of DNA oligonucleotides, a mixture of orange G dye with glycerol in 1:1 ratio was used. With the help of stains-all solution in formamide, the staining of gel was performed. The stained gel was then allowed to place under the white light, where it was photographed to show the acquired bands by Alphalmager™ 2200.

Results and Discussion:

Polyacrylamide Gel Electrophoresis (PAGE)

Denaturating Gel Electrophoresis:

In order to determine the purity of d-TCCCCCAATTAATTCCCCCA (SG20c), denaturating gel electrophoresis was performed. The 20 % denaturating gel was run in a solution

containing 1X TBE along with 100 % formamide (Fig. 1). PAL12 and PAL24 were used as control size marker in Lane 1 and 3, which show the mobility of 12 and 24 nucleotides respectively. On comparing the mobility of SG20c of lane 2 with the used markers, it was inferred that SG20c was moving as a pure single strand.

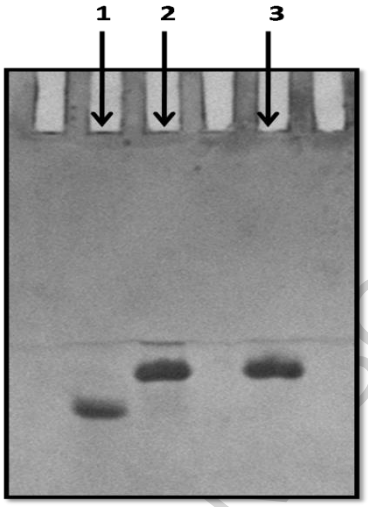

Fig. 1. 20 % denaturating PAGE mobility pattern of DNA oligonucleotide sequences. Lane 1: PAL12, lane 2: SG20c and lane 3: PAL24 in 1X TBE and 100 % formamide.

Native or Non-Denaturating Gel Electrophoresis:

(a). Structural status of C-rich sequences at neutral pH (7.4):

After investigating the purity of C-rich sequence SG20c, non denaturating gel electrophoresis was performed in order to further examine its structural status under varied experimental conditions. 15 % native PAGE was performed at 20 mM sodium cacodylate buffer (pH 7.4) having 0.1 M NaCl and 0.1 mM EDTA (Fig. 2a). PAL12 (12-mer duplex) and PAL24 (24-mer duplex) were used as control size markers to compare the mobility of bands. PAL12 and PAL24 were loaded in lane 1, where they moved as their perfect palindromic duplexes. Beside this, lane 3 comprised of equimolar ratio of both strands SG20 + SG20c and it reflected the mobility as a 40-mer perfect duplex (upper band) and the lower diminished band might be of left over strands of SG20 or SG20c.

A single band was observed for SG20c in lane 2, which was migrating faster than PAL24 but slower than PAL12, on comparative analysis. This mobility pattern indicates the possibility of either an unstructured C-rich strand or an unimolecular species. Exact structural status of SG20c

at 7.4 pH was further explored by employing techniques like UV-thermal melting and CD spectroscopy in the following sections.

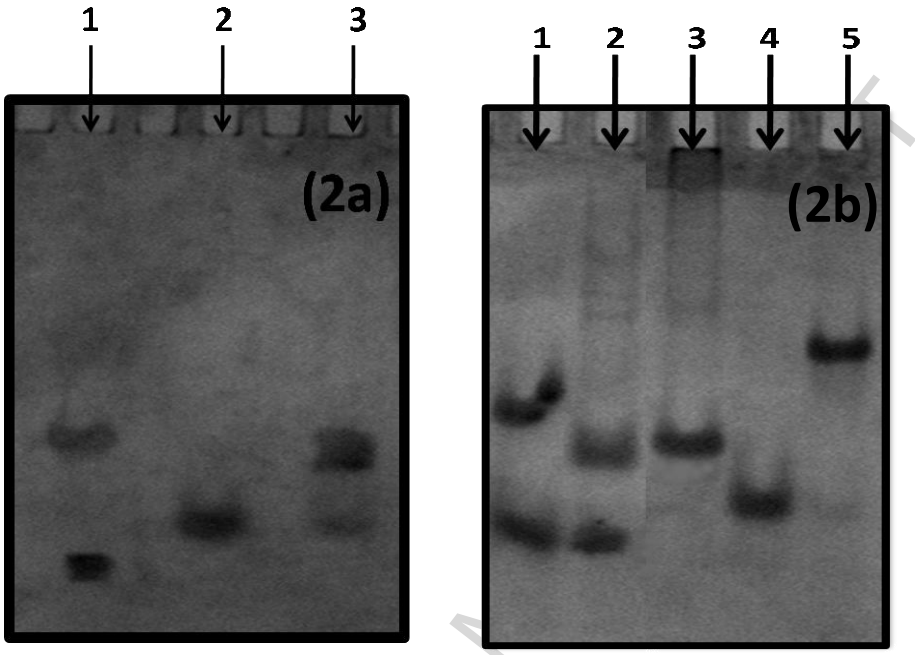

Fig. 2a: 15 % Native PAGE mobility pattern of oligonucleotide sequences. Lane 1: PAL12 + PAL24, lane 2: SG20c, lane 3: SG20 + SG20c, containing 0.1 M NaCl and 0.1 mM EDTA in 20 mM sodium cacodylate buffer (pH 7.4).

Fig. 2b: 15 % Native PAGE mobility pattern of oligonucleotide sequences. lane 1: PAL12 + PAL24, lane 2: SG20c, lane 3: SG20 + SG20c, lane 4: M35, lane 5: M35 + M35C containing 0.1 M NaCl and 0.1 mM EDTA in 20 mM sodium cacodylate buffer (pH 5.2).

(b). Structural status of C-rich sequences at acidic pH (5.2):

At acidic pH, the cytosines get protonated, which are important for the formation of an intercalated motif (i-motif), therefore the gel electrophoresis experiment of SG20c under acidic condition (5.2 pH) was also carried out. The mobility pattern of SG20c in 20 mM sodium cacodylate (pH 5.2) containing 0.1 M NaCl and 0.1 mM EDTA was illustrated in Fig. 2b. Lane 1, lane 4 and lane 5 comprised of control size markers PAL12 (lower band, lane 1), PAL24 (upper band, lane 1), M35 (lane 4) and M35 + M35C (lane 5) respectively. PAL12 and PAL24 are the palindromic sequences which moved as 24 and 48-mer duplex respectively, in non

denaturating conditions. On the other hand, M35 was random sequence, which moved as 35 nucleotides single strand only, whereas an equimolar ratio of M35 + M35c showed the mobility pattern of 70-mer perfect duplex.

Likewise, Lane 2 showed two bands of SG20c and lane 3 showed a single band of SG20 + SG20c in 1:1 stoichiometry. Two bands of SG20C in lane 2 at 5.2 pH indicated the occurrence of two distinct species in the solution. On comparing the mobility with control size markers, the lower band in lane 2 was found to be moving along with PAL12 (running as 24-mer). This fast moving band depicted the possibility of either unstructured oligonucleotide or the formation of unimolecular folded species (intramolecular structure). The retardation in its mobility can be justified by assigning it a folded unimolecular i-motif structure. This structure would further be confirmed by analyzing its CD signatures in following section. Also, the upper band of lane 2 moved equivalent to 40-mer perfect duplex of SG20 + SG20c in lane 3. This suggests that the slow moving band of SG20c might be a bimolecular i-motif structure, which would further be confirmed by CD experiments and UV-thermal denaturation studies, in following sections.

UV-Thermal Denaturation Studies:

To establish the formation of i-motif and to explore their thermal stability, UV-thermal denaturation experiments were performed. It is well documented that at 295 nm, the absorbance decreases in case of i-motif because of increase in base stacking [18]. The occurrence of $C{\bullet}C^+$ base pairs at acidic pH is indicated by decrease in absorbance at 295 nm, hence showing an inverted melting profile. In case of i-motif, these $C{\bullet}C^+$ base pairs are found to be present diagonally over each other in stacking mode. UV-thermal denaturation experiment at 20 mM sodium cacodylate buffer (pH 5.2) containing 0.1 M NaCl and 0.1 mM EDTA was done to investigate the stability of structures formed by SG20c sequence. The melting profile of SG20c at 265 nm and 295 nm along with its first derivatives are displayed in Fig. 3a and 3b**.** The decrease in absorbance (hypochroism) at 295 nm showing inverted melting profile at acidic pH marks the presence of $C{\bullet}C^+$ base pair stabilized i-motif structures [19-21]. The biphasic sigmoidal curve was observed at 265 nm, which was in good agreement with the two bands observed in gel electrophoresis experiment (lane 2 of Fig. 2b.). These two bands and biphasic transitions suggested the possibility of the formation of unimolecular and bimolecular i-motif structures. From the analysis of the first derivative plots for both the structures at 265 nm and

295 nm, identical T_M values were obtained. The upper transition of 63 ^{0}C is attributed to the melting of bimolecular i-motif, while the lower transition of 37 ^{0}C suggested the melting of unimolecular i-motif structure. The higher number of C•C$^+$ base pairs formed in bimolecular i-motif makes it more stable than the unimolecular i-motif (models proposed in fig.5).

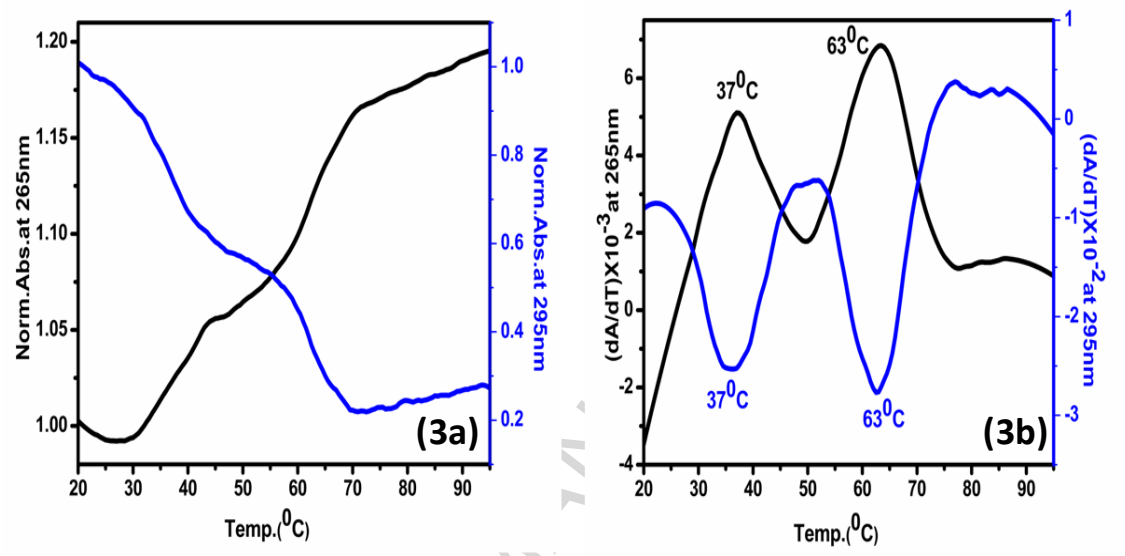

Fig. 3a: Thermal denaturation profiles of SG20c in 20 mM sodium cacodylate buffer (pH 5.2) containing 0.1 M NaCl and 0.1 mM EDTA monitored at 265 nm and 295 nm.

Fig. 3b: First derivatives of thermal melting profiles of Fig. 3a.

Circular Dichroism Studies

CD spectroscopy was employed to explore the conformational status of studied C-rich oligonucleotide SG20c. The characteristic signature of i-motif is marked by a positive peak at around 285-290 nm with a negative band positioned at 260-268 nm [22, 23]. The overlay of CD spectra of SG20c obtained at 20 mM sodium cacodylate (pH 7.4 & 5.2) having 0.1 M NaCl and 0.1 mM EDTA is illustrated in Fig. 4. The spectra at 5.2 pH showed the positive peak centered at 285 nm and a negative band at 252 nm followed by a positive peak at 219 nm, which is a well reported characteristic signature of stacked C•C$^+$ base pairs in i-motif structures. The CD profiles of SG20c at two different pH (7.4 and 5.2) clearly confirm that the formation of i-motif is a pH dependent process. On decreasing the pH from 7.4 to 5.2 of sample solution, a shift in the positive band from 275 to 285 nm has been observed, with an extremely significant increase in

its amplitude. This substantial increment in the amplitude at acidic pH corresponds to the more stable formation of i-motif structures at pH 5.2., in comparison to neutral pH (7.4). A very low CD signal at pH 7.4 indicates that the SG20c sequence remains unstructured single stranded at neutral pH, which was also confirmed by no significant UV-melting profile of the same at pH 7.4 (data not shown).

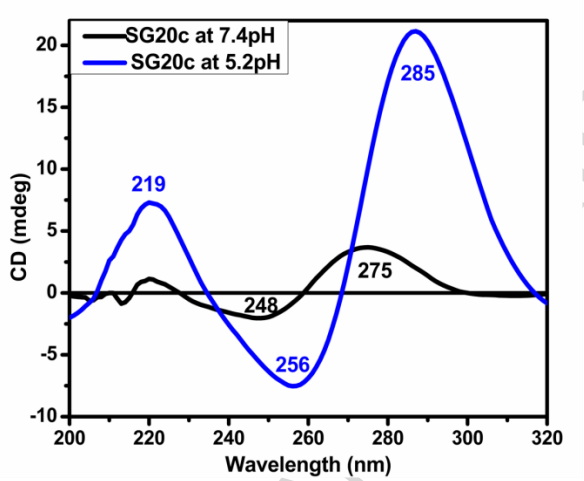

Fig. 4: CD spectra of SG20c in 20 mM sodium cacodylate buffer containing 0.1 M NaCl and 0.1 mM EDTA at pH 7.4 (—) and pH 5.2 (—).

Proposed structural models for unimolecular and bimolecular i-motif structures formed by SG20c at pH 5.2:

After summarizing the results of all experiments done, the structural status of C-rich sequence SG20c at acidic pH, the formation of unimolecular and bimolecular i-motif structures is proposed. Based on experimental investigations and the correlations from gel, CD and $T_{M,}$ formation of three types of i-motif structure seem to be possible, ruling out rest other possibilities. Fig. 5 illustrates all the the proposed structural models for unimolecular and bimolecular i-motif structured adapted by SG20c sequence at acidic pH. Studied sequence SG20c comprised of two CCCCC blocks, in between which $A_2T_2A_2T_2$ is present. The 5'- end has one thymine base, while the 3'- end bears an adenine base. Three possible i-motif structures are proposed, in which one could be unimolecular i-motif and the other two could be bimolecular i-motif having different types of loops.

In unimolecular i-motif, a single oligonucleotide strand of SG20c coils itself in such a way that two C•C^+ base pairs are intercalated at 90 ^{0} between the other C•C^+ base pairs. By doing

so, it forms three consecutive AT base pairs, hence making six hydrogen bonds. Apart from this, adenine at the 3'- end makes two hydrogen bonds with the thymine of 5'- terminal. So if we add, there are eight possible hydrogen bonds in proposed unimolecular i-motif model of SG20c at acidic pH. This unimolecular i-motif structure forms three loops. The loops close to 5'- and 3'- ends have a single cytosine or protonated cytosine base, while the loop in between the extreme ends carry an unpaired A and T base.

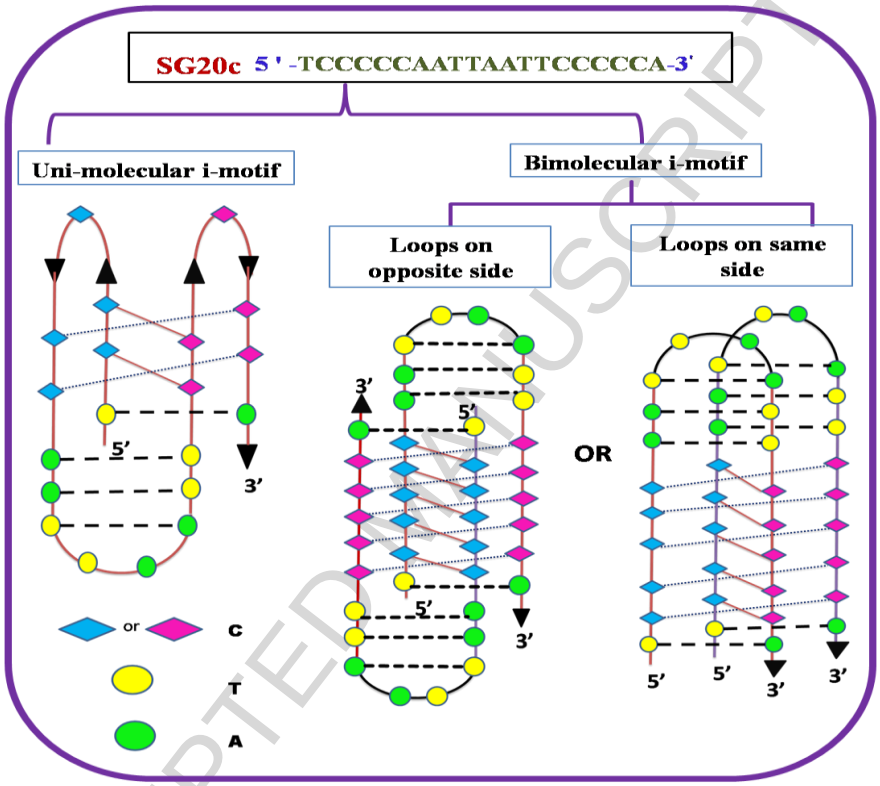

Fig. 5: Proposed model adopted by SG20c at acidic pH.

In case of bimolecular i-motif, two strands of SG20c may assemble to form parallel duplexes, which intercalate in antiparallel orientation, as five C•C$^+$ base pairs are crossing at right angle (diagonal) to another five C•C$^+$ base pairs of another strand. There are two ways by which these dimeric species can arrange themselves: a) having loops on same side, b) having loops on opposite sides. In both the cases, each loop consists of three A-T base pair, resulting in the formation of six hydrogen bonds. In each loop, thymine at 5'- end makes two hydrogen bonds with the adenine at 3' end, so there are sixteen hydrogen bonds present in both the possibilities of bimolecular i-motif structures. Beside this, both the loops in bimolecular i-motif structure have one unpaired A and T base. At this stage, it's not possible for us to discriminate, whether the

bimolecular i-motif formed has both the loops on same side or on opposite side, hence both the possibilities are reported in the illustration (Fig. 5).

Biological Applications:

In recent years, biosensing applications are expanding their potential in research arena because of their significant roles in medicinal diagnosis, biomolecular investigations and analytical studies of molecular pathways. For sensing the environmental conditions, various nanomaterials like quantum dots, metal based nanoparticles and nanotubes have already been synthesized [24-26]. Specific optical, electronic, chemical and mechanical characteristics of these nanomaterials make them suitable devices for reading out the environmental conditions sensitively.

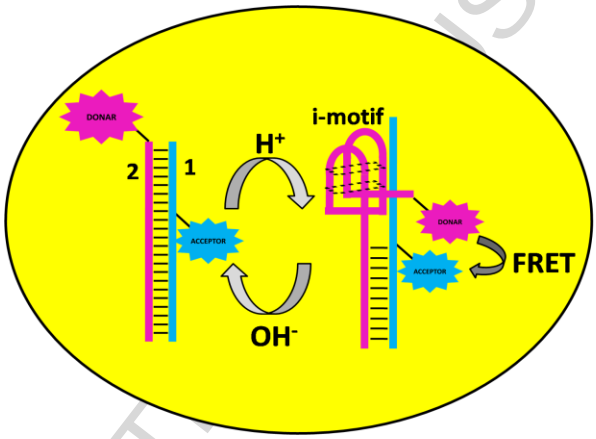

Fig. 6: Mechanism of pH dependent FRET based DNA biosensor. At high pH, FRET remains off as probe 1 and 2 both are hybridized to form DNA duplex, which separate the two attached dyes; Under low pH, probe 2 coils to form i-motif structure, which brings two chromophores in close vicinity and hence the FRET gets on.

DNA, a highly significant biological macromolecule also exhibits it's application as a biosensor. In past few years, DNA had been extensively used in fabrication of two and three dimensional nanoscale lattices [27-29] and complex wire like structures, which have their utilization in medicine [30], biology [31] and material chemistry [32]. The peculiar property of DNA to adopt various conformations in response to varied environmental conditions makes it an efficient and cost effective biosensor. Such biosensor will be functional for a wide range of biologically significant conditions of temperature, pH and chemical environment [33-37].

The branch of DNA nanotechnology has been exhibiting lots of promising applications in the manufacturing of DNA based machines [38, 39], which can respond by change in environmental conditions. Biosensors depend on the specific recognition of change in environmental stimuli (such as change in pH) by the DNA molecule. An example of the mechanism of FRET based biosensor, utilizing the formation of i-motif structure for bio recognition has been depicted in Fig. 6.

Likewise, as an example of structure-specific recognition, it has recently been reported that two ligands/ molecules named IMC-76 and IMC-48 stabilize hairpin and i-motif conformations respectively [40]. The binding of hnRNP LL transcription factor is structure specific, which facilitates its binding with i-motif, while prohibiting its binding to hairpin conformation and thereby suppressing and activating the transcription of Cancer cells respectively illustrated in Fig. 7.

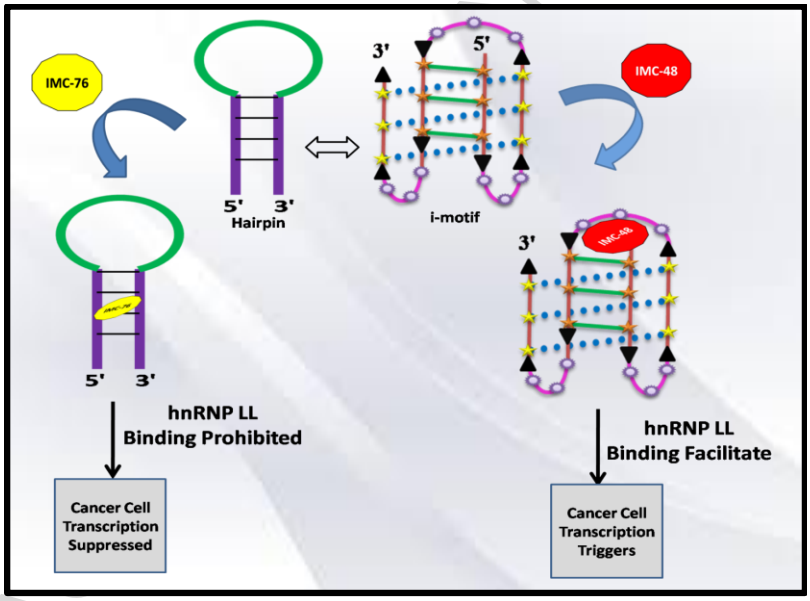

Fig. 7: Structure-specific recognition of hairpin and i-motif by small ligands, showing suppression and activation of the transcription of cancer cells

An intermolecular interaction of logically proposed DNA sequence with its environment enables us to construct nanoparticles of definite morphology. Large number of nucleic acid based biosensors include hybridization of DNA or RNA. The hairpin conformation of nucleic acid (DNA or RNA) can be used to analyze the change in environmental condition such as

temperature by tagging the ends of the strand with a fluorophore-quencher pair. The stimuli such as change in pH are more efficient in converting the single stranded DNA into triplex and i-motif structure and setting a good example of pH dependent sequence specific biosensor [41]. Another example of sequence specific biosensor is G-quadruplex formation by guanine-rich DNA sequences, which takes place under particular ionic condition such as in presence of K^+ or Na^+ ions [42]. Beside this DNA as biosensor can also respond to aptamer recognition. Aptamers are the small single stranded oligonucleotide which exhibit a good binding affinity for small organic moieties, ions, proteins and microorganisms and results into secondary structure formation [43, 44].

Conclusions:

In this study, by correlating the results obtained from UV-melting, non-denaturating polyacrylamide gel electrophoresis, and circular dichroism experiments, the structural status of a cytosine-rich oligonucleotide d(TCCCCCAATTAATTCCCCCA) [SG20c] has been determined at different pH conditions. From the electrophoretogram obtained by PAGE experiment, two species were observed, which were assigned the status of unimolecular and bimolecular i-motif structures. UV-thermal denaturation profile at 5.2 pH also exhibited biphasic melting transitions both at 265 nm and 295 nm wavelength, confirming the formation of two i-motif structures. Depending upon the stability, the lower temperature transition was attributed to intramolecular/ unimolecular i-motif, while the higher melting temperature was attributed to intermolecular bimolecular i-motif structure. As from the proposed models, it is observed that more number of hydrogen bonds and $C•C^+$ base pairs are possible in bimolecular i-motif, making it more stable in comparison to unimolecular i-motif. Further by employing CD spectroscopy, the conformational status of these structures as i-motif has been confirmed. The CD spectra at acidic pH showed a positive peak at 285 nm along with a negative peak around 256 nm, which are the characteristic signatures of the i-motif conformation. Since DNA structure seems to be a potential biocompatible biosensing device, which can be tuned in desired nanoscale dimensions, hence studies like this which are based on conformational polymorphism of DNA structures become quite significant.

Acknowledgment:

The authors acknowledge the Research and Development (R & D) grant from University of Delhi. SA thanks Delhi University for the grant of the research Fellowship to her.

REFRENCES:

1) J.D. Watson, F.H. Crick, Molecular structure of nucleic acids, Nature. 171(4356) (1953) 737-738.
2) J. Choi, T. Majima, Conformational changes of non-B DNA, Chem. Soc. Rev. 40(12) (2011) 5893-5909.
3) J.L. Huppert, Structure, location and interactions of G-quadruplexes, FEBS J. 277(17) (2010) 3452-3458.
4) R. Rodriguez, K.M. Miller, J.V. Forment, C.R. Bradshaw, M. Nikan, S. Britton, et al., Small-molecule–induced DNA damage identifies alternative DNA structures in human genes, Nat. Chem. Biol. 8(3) (2012) 301-310.
5) G. Biffi, D. Tannahill, J. McCafferty, S. Balasubramanian, Quantitative visualization of DNA G-quadruplex structures in human cells, Nat. Chem. 5(3) (2013) 182-186.
6) K. Gehring, J.L. Leroy, M. Guéron, A tetrameric DNA structure with protonated cytosine-cytosine base pairs, Nature. 363(6429) (1993) 561-565.
7) M. Kaushik, M. Prasad, S. Kaushik, A. Singh, S. Kukreti, Structural transition from dimeric to tetrameric i-motif, caused by the presence of TAA at the 3′-end of human telomeric C-rich sequence, Biopolymers. 93(2) (2010) 150-160.
8) D. Liu, S. Balasubramanian, A Proton-Fuelled DNA Nanomachine, Angew. Chem. Int. Ed. 42(46) (2003) 5734-5736.
9) Z.G. Wang, J. Elbaz, I. Willner, DNA machines: bipedal walker and stepper, Nano Lett. 11(1) (2010) 304-309.
10) W. Wang, H. Liu, D. Liu, Y. Xu, Y. Yang, D. Zhou, Use of the interparticle i-motif for the controlled assembly of gold nanoparticles, Langmuir. 23(24) (2007) 11956-11959.
11) J. Sharma, R. Chhabra, H. Yan, Y. Liu, pH-driven conformational switch of “i-motif” DNA for the reversible assembly of gold nanoparticles, Chem. Commun. 5 (2007) 477-479.

12) J. Elbaz, Z.G. Wang, R. Orbach, I. Willner, pH-stimulated concurrent mechanical activation of two DNA "tweezers". A "SET− RESET" logic gate system, Nano Lett. 9(12) (2009) 4510-4514.

13) Y. Yang, G. Liu, H. Liu, D. Li, C. Fan, D. Liu, An electrochemically actuated reversible DNA switch, Nano Lett. 10(4) (2010) 1393-1397.

14) T. Li, D. Ackermann, A.M. Hall, M. Famulok, Input-dependent induction of oligonucleotide structural motifs for performing molecular logic, J. Am. Chem. Soc. 134(7) (2012) 3508-3516.

15) S. Modi, M.G. Swetha, D. Goswami, G.D. Gupta, S. Mayor, Y. Krishnan, A DNA nanomachine that maps spatial and temporal pH changes inside living cells, Nat. Nanotechnol. 4(5) (2009) 325-330.

16) S. Surana, J.M. Bhat, S.P. Koushika, Y. Krishnan, An autonomous DNA nanomachine maps spatiotemporal pH changes in a multicellular living organism, Nat. Commun. 2 (2011) 340.

17) C.R. Cantor, M.M. Warshaw, H. Shapiro, Oligonucleotide interactions. III. Circular dichroism studies of the conformation of deoxyoligonucleolides, Biopolymers. 9(9) (1970) 1059-1077.

18) J.L. Leroy, J.L. Mergny, M. Gueron, C. Helene, Intramolecular folding of a fragment of the cytosine-rich strand of telomeric DNA into an i-motif, Nucleic Acids Res. 22 (1994) 1600-1606.

19) G. Manzini, N. Yathindra, L.E. Xodo, Evidence for intramolecularly folded i-DNA structures in biologically relevant CC-repeat sequences, Nucleic Acids Res. 22 (1994) 4634-4640.

20) M. Gueron, L. Leroy, The i-motif in nucleic acids, Curr. Opin. Struct. Biol. 10 (2000) 326-331.

21) J.L. Mergny, L. Lacroix, Kinetics and thermodynamics of i-DNA formation: phosphodiester versus modified oligodeoxynucleotides, Nucleic Acids Res. 26 (1998) 4797–4803.

22) G. Manzini, N. Yathindra, L.E. Xodo, Evidence for intramolecularly folded i-DNA structures in biologically relevant CC-repeat sequences, Nucleic Acids Res. 22 (1994) 4634-4640.

23) H. Kanehara, M. Mizuguchi, K. Tajima, K. Kanaori, K. Makino, Spectroscopic evidence for the formation of four-stranded solution structure of oligodeoxycytidine phosphorothioate, Biochem. 36 (1997) 1790-1797.

24) T. Ahuja, D. Kumar, Recent progress in the development of nano-structured conducting polymers/ nanocomposites for sensor applications, Sens. Actuator B-Chem. 136(1) (2009) 275-286.

25) J. Lei, H. Ju, Signal amplification using functional nanomaterials for biosensing, Chem. Soc. Rev. 41(6) (2012) 2122-2134.

26) Y. Zhang, Y. Guo, Y. Xianyu, W. Chen, Y. Zhao, X. Jiang, Nanomaterials for ultrasensitive protein detection, Adv. Mater. 25(28) (2013) 3802-3819.

27) W. Wang, T. Lin, S. Zhang, T. Bai, Y. Mi, B. Wei, Self-assembly of fully addressable DNA nanostructures from double crossover tiles, Nucleic Acids Res. 44(16) (2016) 7989-7996.

28) J. Zheng, J.J. Birktoft, Y. Chen, T. Wang, R. Sha, P.E. Constantinou, et al. From molecular to macroscopic via the rational design of a self-assembled 3D DNA crystal, Nature. 461(7260) (2009) 74.

29) D. Bhatia, S. Arumugam, M. Nasilowski, H. Joshi, C. Wunder, V. Chambon, et al., Quantum dot-loaded monofunctionalized DNA icosahedra for single-particle tracking of endocytic pathways, Nat. Nanotechnol. 11(12) (2016) 1112-1119.

30) R. Chhabra, J. Sharma, Y. Liu, S. Rinker, H. Yan, DNA self-assembly for nanomedicine, Adv. Drug Deliv. Rev. 62(6): (2010) 617-625.

31) A. Czogalla, H.G. Franquelim, P. Schwille, DNA Nanostructures on Membranes as Tools for Synthetic Biology, Biophys. J. 110(8) (2016) 1698-1707.

32) C.M. Niemeyer, Nanoparticles, proteins, and nucleic acids: biotechnology meets materials science, Angew. Chem. Int. Ed. 40(22) (2001) 4128-4158.

33) J. Chao, D. Zhu, Y. Zhang, L. Wang, C. Fan, DNA nanotechnology-enabled biosensors, Biosens. Bioelectron. 76 (2016) 68-79.

34) H.M. Meng, H. Liu, H. Kuai, R. Peng, L. Mo, X.B. Zhang, Aptamer-integrated DNA nanostructures for biosensing, bioimaging and cancer therapy, Chem. Soc. Rev. 45(9) (2016) 2583-2602.

35) A.R. Chandrasekaran, H. Wady, H.K. Subramanian, Nucleic acid nanostructures for chemical and biological sensing, Small. 12(20) (2016) 2689-2700.

36) H. Pei, X. Zuo, D. Pan, J. Shi, Q. Huang, C. Fan, Scaffolded biosensors with designed DNA nanostructures, NPG Asia Mater. 5 (2013) e51.

37) A. R. Chandrasekaran , DNA Nanobiosensors: An Outlook on Signal Readout Strategies, J Nanomater. 2017.

38) J. Bath, A. J. Turberfield, DNA nanomachines, Nat. Nanotechnol. 2(5) (2007) 275-284.

39) F.C. Simmel, W.U. Dittmer, DNA nanodevices, Small. 1(3) (2005) 284-299.

40) S. Kendrick, H. J. Kang, M. P. Alam, M.M. Madathil, P. Agrawal, V. Gokhale, et al., The dynamic character of the *BCL2* promoter i-motif provides a mechanism for modulation of gene expression by compounds that bind selectively to the alternative DNA hairpin structure, J. Am. Chem. Soc. 136 (2014) 4161−4171.

41) S. Chakraborty, S. Sharma, P.K. Maiti, Y. Krishnan, The poly dA helix: a new structural motif for high performance DNA-based molecular switches, Nucleic Acids Res. 37(9) (2009) 2810-2817.

42) S.Burge, G.N. Parkinson, P. Hazel, A.K. Todd, S. Neidle, Quadruplex DNA: sequence, topology and structure, Nucleic Acids Res. 34(19) (2006) 5402-5415.

43) S. Song, L. Wang, J. Li, C. Fan, J. Zhao, Aptamer-based biosensors, Trends Anal. Chem. 27(2) (2008) 108-117.

44) S. Tombelli, M. Minunni, M. Mascini, Analytical applications of aptamers, Biosens. Bioelectron. 20(12) (2005) 2424-2434.